On sloshing modes in square or nearly square moonpools

Bernard Molin

Aix Marseille Univ, CNRS, Centrale Marseille, IRPHE, Marseille, France
Bureau Veritas Marine & Offshore SAS, 67/71 Boulevard du Château, 92571 Neuilly sur Seine
Dept of Marine Technology, Norwegian University of Science and Technology NTNU, Trondheim
bernard.molin@centrale-marseille.fr

Consider a rectangular tank of length L, width B, filled with water to a height h. The natural sloshing modes in the tank are

$$\varphi_{mn} = \frac{\cosh \nu_{mn} z}{\cosh \nu_{mn} h} \cos \lambda_m x \; \cos \mu_n y \tag{1}$$

where the coordinate center has ben taken at one of the lower corners and $\lambda_m = m\,\pi/L$, $\mu_n = n\,\pi/B$, $\nu_{mn}^2 = \lambda_m^2 + \mu_n^2$. Each geometric mode (m,n) is a natural mode with frequency ω_{mn} given by $\omega_{mn}^2 = g\,\nu_{mn}\,\tanh \nu_{mn} h$. When the tank is square then the natural frequencies ω_{mn} and ω_{nm} collapse to the same values.

In a rectangular moonpool a natural sloshing mode consists in the superimposition of several geometric modes (m,n), one of which is usually dominant over the others. Recently Molin *et al.* (2017) have extended the original theory of Molin (2001) to finite depth and considered, as a validation case, among others, a square moonpool proposed by Ideol as a floating windmill foundation (Guignier *et al.* 2016). There it has been found that the natural frequencies ω_{20} and ω_{02} do not collapse to the same value. In this paper we more deeply investigate the issue.

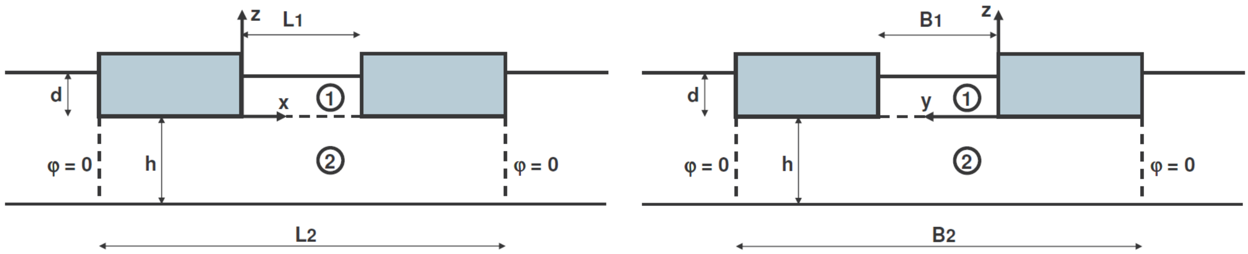

Figure 1: Geometry.

Fig. 1 shows the geometry of the problem. The inner fluid domain is divided into two sub-domains: the moonpool, and a lower sub-domain bounded by the keel, the sea-floor and a vertical cylinder where the velocity potential is taken to be nil. This is a gross condition to ensure matching with the outer fluid domain, however it has been found to provide valuable results (Molin *et al.* 2017).

Alike in Molin (2001), the velocity potential in sub-domain 1 (the moonpool) is taken as

$$\varphi_1(x,y,z) = A_{00} + B_{00}\,\frac{z}{d} + \sum_{m=0}^{\infty} \sum_{\substack{n=0 \\ (m,n)\neq(0,0)}}^{\infty} \left[A_{mn}\,\cosh \nu_{mn} z + B_{mn}\,\sinh \nu_{mn} z\right] \,\cos \lambda_m x \;\cos \mu_n y \tag{2}$$

with

$$\lambda_m = m\,\pi/L_1 \qquad \mu_n = n\,\pi/B_1 \qquad \nu_{mn}^2 = \lambda_m^2 + \mu_n^2 \tag{3}$$

In the lower sub-domain it is

$$\varphi_2(x,y,z) = \sum_{p=1}^{\infty}\sum_{q=1}^{\infty} C_{pq}\,\frac{\cosh \gamma_{pq}(z+h)}{\cosh \gamma_{pq} h}\; \sin \alpha_p(x+a)\; \sin \beta_q(y+b) \tag{4}$$

with

$$\alpha_p = p\,\pi/L_2 \qquad\qquad \beta_q = q\,\pi/B_2 \qquad\qquad \gamma_{pq}^2 = \alpha_p^2 + \beta_q^2 \tag{5}$$

p and q integers, and $a = (L_2 - L_1)/2$, $b = (B_2 - B_1)/2$.

By equating φ_1 and φ_2 (and their vertical derivatives) on the common boundary (and ensuring the no-flow condition $\partial\varphi_2/\partial z = 0$ on the hull), a vectorial equation in the form $\overrightarrow{A} = \mathbf{AB} \cdot \overrightarrow{B}$ can be derived. The following steps are then identical with Molin (2001), i.e. solving an eigen-value problem for $\overrightarrow{B}$ and obtaining the natural frequencies and associated modal shapes. An advantage of the new model as compared to the previous one is that it is much cheaper to run numerically (there is no need to compute complicated double integrals).

We take the same moonpool dimensions as in Guignier *et al.* (2016), that is 27 m $\times$ 27 m, the same waterdepth (55 m), but we decrease the draft to 3 m. As for the outer vertical cylinder we take $L_2 = B_2 = 81$ m.

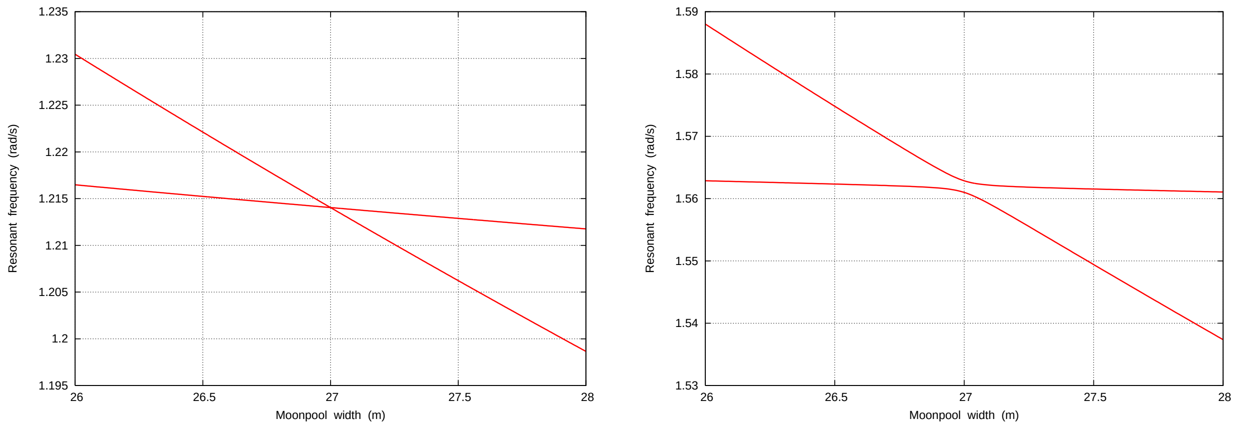

Figure 2: First (left) and second (right) sloshing modes. Natural frequencies.

In one run of the numerical model we get a discrete set of natural frequencies which we range in increasing values. The lowest value corresponds to the piston mode, then come the first sloshing modes dominated by the geometric modes (1,0) and (0,1), then the diagonal mode (1,1), then the second sloshing modes that involve the geometric modes (2,0) and (0,2).

We keep all geometric parameters as written above, and we vary the width B_1 from 26 m to 28 m. Fig. 2 shows the natural frequencies obtained for the first sloshing modes (left) and for the second sloshing modes (right). Considering first the left figure, it can be seen that the two curves intersect at $B_1 = 27$ m: when the moonpool is square the two modes coalesce to the same frequency. Looking now at the right figure, it can be seen that it is not the case for the second modes: there are two distinct frequencies in the square case and the curves do not intersect.

As written above, when the moonpool is rectangular, each natural mode is dominated by one geometric mode. Fig. 3 shows the geometric modes (m, n) that contribute to the the second sloshing modes. The contributions are normalized by a maximum value of one. The left figure is for the lower branch in Fig. 2b, the right figure is for the upper branch. As the moonpool becomes square, it can be seen that both geometric modes (2,0) and (0,2) contribute, ultimately with the same absolute value. At the lowest of the two frequencies, they add up algeabrically, at the highest one they subtract. A small contribution from the geometric mode (0,0) can also be seen.

Figures 4 through 10 show the evolutions of the modal shapes of the free surface elevation as the width goes from 26.5 m to 27.5 m. The left column is for the lower branch in Fig. 2b, the right column for the upper branch. It can be seen that the longitudinal sloshing mode continuously transforms into the transverse sloshing mode, and vice versa.

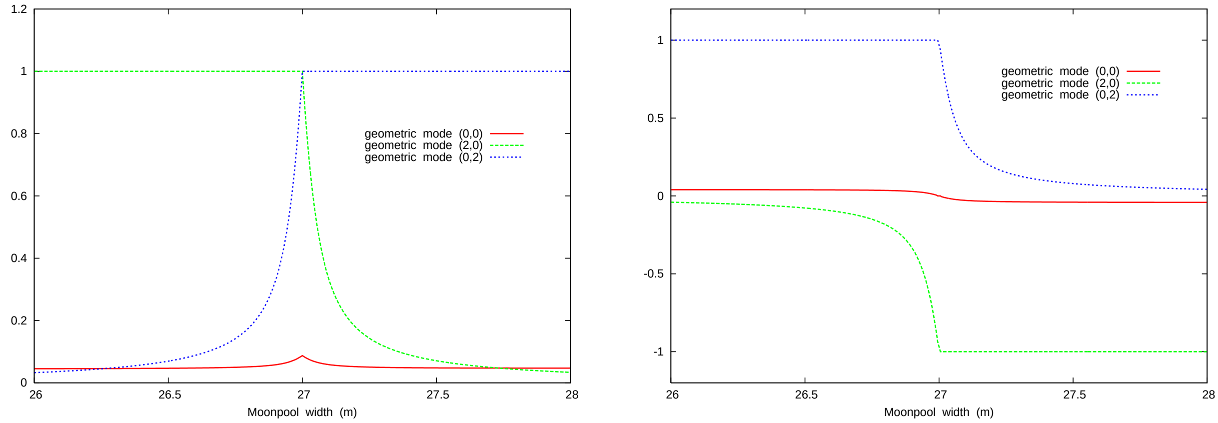

Figure 3: Participation of the geometric modes (m, n) to the second sloshing modes.

References

Guignier L., Courbois A., Mariani R. & Choisnet T. 2016 Multibody Modelling of Floating Offshore Wind Turbine Foundation for Global Loads Analysis, in *Proc. of the Twenty-sixth (2016) International Ocean and Polar Engineering Conference*, Rhodes.

Molin B. 2001 On the piston and sloshing modes in moonpools, *J. Fluid Mech.*, **430**, 27–50.

Molin B., Zhang X., Huang H. & Remy F. 2017 On natural modes in moonpools and gaps in finite depth, submitted.

Figure 4: Width 26.5 m.

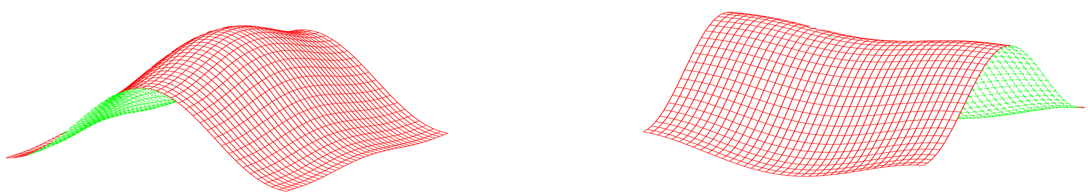

Figure 5: Width 26.8 m.

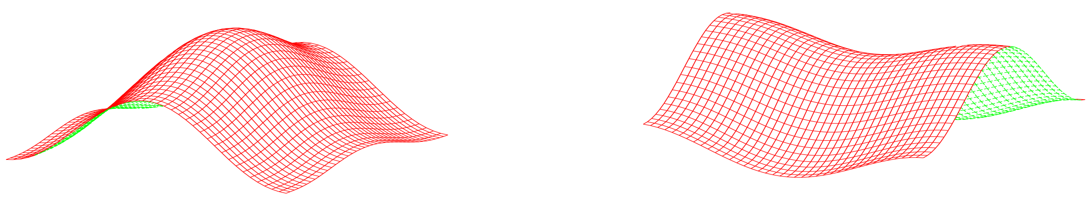

Figure 6: Width 26.9 m.

Figure 7: Width 27 m.

Figure 8: Width 27.1 m.

Figure 9: Width 27.2 m.

Figure 10: Width 27.5 m.